MAGNETIC RESONANCE IN MEDICINE 3, 823–833 (1986)

RARE Imaging: A Fast Imaging Method for Clinical MR

J. HENNIG,*A. NAUERTH,† AND H. FRIEDBURG*

*Department of Diagnostic Radiology, University Hospital, University of Freiburg, Hugstetter Strasse 55, West Germany, and †Bruker Medizintechnik GmbH, POB 67, 7512 Rheinstetten-4/West Germany

Received May 6, 1985; revised April 14, 1986

Based on the principles of echo imaging, we present a method to acquire sufficient data for a 256 × 256 image in from 2 to 40 s. The image contrast is dominated by the transverse relaxation time T_2. Sampling all projections for 2D FT image reconstruction in one (or a few) echo trains leads to image artifacts due to the different T_2 weighting of the echo. These artifacts cannot be described by a simple smearing out of the image in the phase direction. Proper distribution of the phase-encoding steps on the echoes can be used to minimize artifacts and even lead to resolution enhancement. In spite of the short data acquisition times, the signal amplitudes of structures with long T_2 are nearly the same as those in a conventional 2D FT experiment. Our method, therefore, is an ideal screening technique for lesions with long T_2.

Conventional imaging techniques used in MRI take several minutes for a multislice and/or multiecho 256 × 256 image. The use of these time-consuming methods causes several problems in routine clinical work. These well known problems include patient discomfort and positioning—especially when one is looking for small lesions and image artifacts due to patient movement.

It would therefore be of great importance to have an imaging method that allows a more rapid data acquisition. Although one is willing to pay some price in image quality for such a faster image, the image has to fulfill several conditions to be of any help in the problems mentioned above. The resolution should not be worse than that of a normal image, the image contrast should be variable and good enough to distinguish normal tissue from lesions, and of course the signal-to-noise ratio should be good enough to deliver an acceptable image quality. Above that, the imaging method should use only rf field strength, gradient field strength, and rising times which lay well within the limits given by the national health organizations (*1*).

There are several methods that lead to faster imaging. The standard menu of most of today's clinical MRI systems allows the fast acquisition of a low-resolution (128 × 256) image by simply reducing the repetition time of a single-slice single-echo experiment. Since in such an experiment practically all the magnetization is very heavily saturated, the resulting image has very low S/N and contrast. Better results can be achieved by performing the experiment using excitation pulses with smaller flip angle (*2–4*). Although this leads to much better S/N and contrast, these methods still lack sensitivity for structures with long relaxation times, which are the ones most sought after in clinical MRI, especially in head investigations.

The method we pursued is based on the principle of echo imaging, first introduced

0740-3194/86 $3.00

to MRI by Mansfield (*5–7*). Long echo trains are generated whereby each echo is encoded differently for spatial coordinates (Fig. 1). Applied to 2D FT, where one axis of the imaged plane is represented by the phase information of the echoes, this means, that all other sources affecting the phase of the echoes have to be dealt with adequately. Disastrous phase errors can be introduced by H_1, H_0, and switched gradient field inhomogeneities. Sampling data very fast minimizes magnetic field effects, as has been shown by Mansfield (*5–7*). Although a MR–real-time movie could be demonstrated with this method, its routine application is restricted since the gradient field strength necessary lies outside the possibilities of routine MRI systems.

Several methods to overcome inhomogeneities by self-compensating spin-echo sequences have been proposed (*8–10*), but, due to the fact that only some inhomogeneities were accounted for, only a modest approximation to a clinical fast imaging sequence could be achieved (*10, 11*). The problem can be solved by respecting the CPMG conditions regarding the phase of the magnetization not only in respect to the phase of the transmitter signals but to the switched gradient fields as well (*12*). This means, all gradient effects are compensated within one echo cycle, so that no accumulative effects can arise. There are different ways this principle can be incorporated into a working pulse program (*13, 18*). This enables the data acquisition with only a few—in the limiting case one—excitations of the spin system.

IMAGE QUALITY

The data flow in the 2D FT image reconstruction algorithm can be characterized by

$$E \xrightarrow{\text{FT}} F \longrightarrow E' \xrightarrow{\text{FT}} S.$$

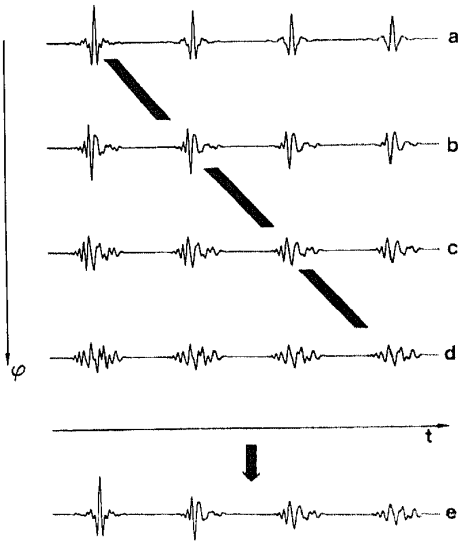

FIG. 1. Principle of echoimaging. (a–d) show 4 echo trains of a conventional 2D FT experiment. Each echotrain carries different phase encoding φ. In the echo imaging experiment only one echo train is sampled, the phase encoding is different for each echo.

Echoes E are sampled in the time domain, their Fourier transforms F are rearranged to give the "echoes" E', which yield the shape function S after the second FT. In a conventional 2D FT experiment all projections necessary for image reconstruction are read out at the same time after excitation. Contrary to that, each projection in an echoimaging experiment is read out at a different time and therefore experiences a different attenuation due to T_2 relaxation. To evaluate the quality of the image measured by this method one has to know how this affects the image contrast.

An easy approach to this problem is to consider first a conventional 2D FT experiment performed on a point-like object located at the center of the gradient system. Due to its location this object experiences no influence due to gradients whatsoever and all echoes E are characterized by frequency zero and an amplitude that is proportional to the product of the spin density with the value of the T_2 relaxation function at the echo readout time. The Fourier transform yields identical delta functions at the origin. Rearrangement of the data matrix according to the 2D FT algorithm yields "echoes" E', all of which are zero except one, which again is characterized by frequency zero. The second Fourier transform yields the set of shape functions S, all of which are zero except the one at the center, which again is given by a delta function. The resulting image shows intensity only in the voxel at the center.

If an echoimaging experiment is performed on this trivial case, all echoes are again characterized by frequency zero. The amplitude, however, is now different in all projections due to T_2 relaxation. This means, that after the first Fourier transform one gets a set of delta functions with different amplitudes. The result after rearrangement and second Fourier transform strongly depends on the pattern of the data sampling. If the dephasing steps are distributed stochastically on the echoes of the echotrain, the result is a noise-like pattern for the "echo" E', the corresponding image consists of a point in the center due to the fact, that all values of E' are greater zero, plus many artifacts randomly distributed along the central line of the image.

A more rational approach would be a sequential distribution of the phase-encoding steps on the echo train. In this case the "echo" E' looks like a discrete representation of the T_2 relaxation function of the object. The time interval between two sampling points is given by the echo spacing $2*\tau_e$. The resulting shape function consists of a Lorentzian line, whose width is determined by the relaxation time T_2. The image appears to be smeared out in the phase direction, the smearing being more severe for short T_2 and/or long echo spacing $2*\tau_e$.

If an echo imaging experiment is performed that delivers coherent echoes in the manner described in the previous chapter, then the outcome of the experiment is not altered by the addition of gradients. This means, that independent of its location, a point-like object always yields an image, which is smeared out somewhat in the phase direction (*14*).

The complementary case is that of an image with infinite extension. Here E' is given by a delta function whose amplitude is solely defined by the amplitude of the projection with zero dephasing, since this is the only one with nonzero intensity. The resulting image is a grey plane with homogeneous intensity, the intensity value is given by the product of the spin density with the value of the relaxation function at the readout time of that particular echo. In general, objects with short relaxation times will appear darker than those with long relaxation times at equal spin density.

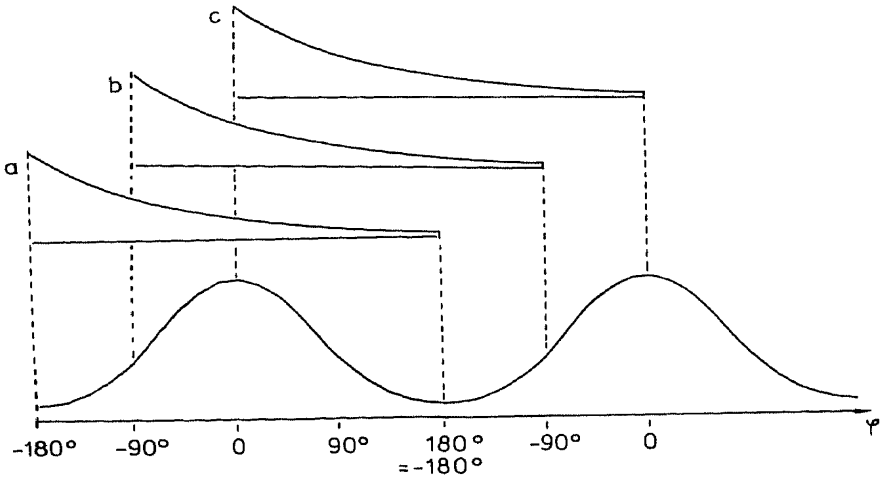

FIG. 2. The "echo" E' as yielded after the first half of the 2D FT algorithm. The horizontal scale gives the relative phaseshift of neighboring voxels due to phase encoding. For clarity two cycles of E' are shown. In an echo imaging experiment E' is multiplied by the relaxation function. Three possibilities differing in the sequence of phase-encoding steps are represented by (a–c).

A somewhat more realistic situation arises if one looks at objects with finite extension inside the image frame and characterized by one relaxation function. The result of an echo imaging experiment for such a case is shown qualitatively in Figs. 2 and 3. Figure 2 shows the "echo" E' as a result of the first Fourier transform and rearrangement of the data matrix in a conventional 2D FT experiment. E' is cyclic in the sense that a phase difference of $-180°$ between neighboring points yields the same result as a phase difference of 180° according to the aliasing principle in discreet Fourier transformation. For the sake of the following argument, two cycles of E' are shown. As described above, this "echo" has to be multiplied by the discreet representation of the relaxation

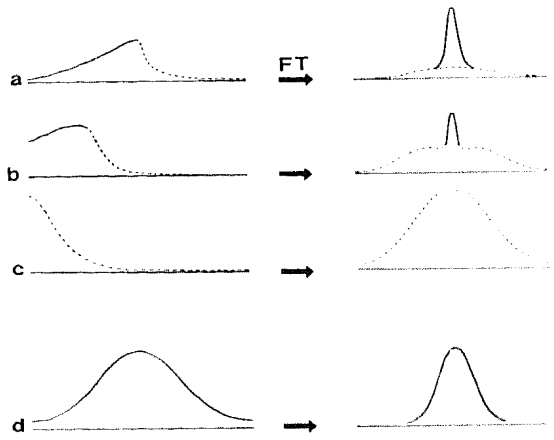

FIG. 3. The result of experiments 2a–c. The resolution of the final shape functions S (right) strongly depend on the way of phase encoding. S can appear even to be resolution enhanced as compared to the result of a conventional 2D FT (d). The effects are exaggerated in these purely qualitative drawings.

function, if an echo imaging experiment is performed, where the phase-encoding steps are distributed sequentially. The outcome of this experiment depends not only on the fact that the phase-encoding steps are distributed sequentially on the echoes, but also on which phase is attributed to the first echo, that is, where the experiment starts in the phase cycle. Three cases are shown in Figs. 2a–c. Figure 3 shows the final result after the second Fourier-transform. Figure 3d shows the shape function as yielded in a conventional 2D FT experiment. Figures 3a–c show the strong dependence of the result on the exact manner of distributing the phase-encoding steps. It is particularly interesting to note, that the shape can appear to be sharpened (Fig. 3a), contrary to what one would expect by a simplistic generalization of the argument for point-like objects.

This sharpening can be rationalized if E' is separated into an ascending part and a descending part. Multiplying the ascending part with the monotonous descending relaxation function leads to a flatter slope and therefore to a sharpening after Fourier transformation. Multiplication of the descending part (shown in dotted line in Figs. 3a–c) yields an even steeper slope and broadening after Fourier transformation. The shape function S is the sum of both parts.

According to the basic properties of Fourier transformation the center (= zero frequency) amplitude of the shape function is given by the integral of E' after multiplication with the discreet representation of the relaxation function. It is therefore dependent on T_2 and $2*\tau_e$ as well as on the exact shape of the object and the manner of phase encoding.

The slope of the discreet representation of the relaxation function depends not only on T_2, but also on the echo spacing $2*\tau_e$. Shorter echo spacing leads to a more gradual slope and therefore to a less pronounced effect on the amplitude of the shape function as well as its distortion.

Due to technical restrictions, $2*\tau_e$ cannot be made arbitrarily small in a multiecho experiment. An artificial shortening of the sampling steps for the relaxation function can be achieved if the experiment is performed with n excitations instead of one and the phase-encoding steps are interleaved (*15*). Discontinuities arising from the fact that by simple repetition of the multiecho experiment under variation of the phase-encoding groups of n projections are sampled at identical readout times, can be removed by one of the following methods:

(1) Prolongation of the times between 90° and the first 180° pulse by τ_e/n in consecutive echo trains.

(2) Substitution of the 90° pulse by a 90°–τ_e/n–180° pulse sequence.

(3) Substitution of the 90° pulse by a 90° pulse followed by an orthogonal spin-locking pulse of duration τ_e/n.

For an explicit calculation for a realistic case, the image representing spin density has first to be separated into regions with identical T_2. E' has to be calculated for all those shape functions by inverse Fourier transformation and the multiplication according to the phase-encoding scheme carried out using the appropriate discreet representation of the respective relaxation functions. Fourier transformation and addition of the results for all different T_2's leads to the echo image.

Of course such a calculation is impracticable for a clinical case. Some insight can

however be gained by looking at the result of the explicit calculation for objects with Lorentzian spin-density distribution along the phase direction, which is given in the Appendix. Figures 4a–d show the influence of T_2 and the width of a structure on the signal intensity for a single-excitation echo image and one that used 16 excitations in the manner described above. It is clear, that the relaxation constant is the main determining parameter for the intensity attenuation (Figs. 4a, b). We therefore call this method RARE imaging for Rapid Acquisition with Relaxation Enhancement.

Figure 4b shows that the T_2 contrast is much less pronounced if one samples the data in 16 echotrains with 16 echoes each, leading to a good presentation of even short T_2 structures. The influence of the width of the structure is shown in Figs. 4c–d. Sharp structures are more attenuated than structures with medium width. Not shown in the graphs is the sharp decline of the signal intensity for very broad structures especially when the dephasing zero point is put into late echoes.

A very interesting point to note is given by the second vertical scale in Figs. 3 and 4. It gives the signal sampled per unit of time as compared to a conventional 2D FT experiment and therefore can be used as a measure of the efficiency of the imaging method. For structures with long T_2, this figure of merit can be as high as 100, clearly contradicting the common misconception, that faster imaging for a given resolution is only attainable at the cost of low signal to noise.

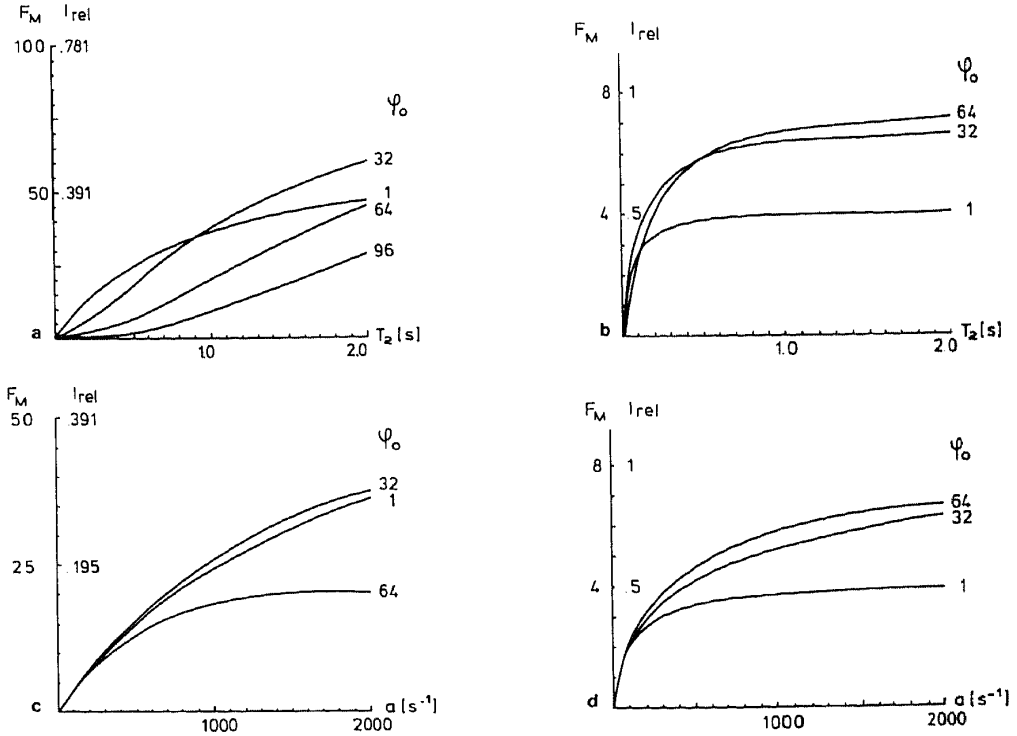

FIG. 4. Calculated relative intensities for Lorentzian shapes in a 256 × 256 RARE image. The intensity units I_{rel} are scaled to 1 equal to the spin density. Figure of merit F_M is given as the quotient of Signal sampled per unit of time for RARE image divided by the same number for a conventional 2D FT image with same resolution. (a) I vs T_2 for a single-shot image; (b) I vs T_2 for a 16-excitation image; (c) I vs a for a single-shot image; (d) I vs a for 16-excitation image where a is the linewidth of the Lorentzian shape in Hz for a total image size of 25 kHz. φ_0 gives the echo number with dephasing gradient 0.

RESULTS

The validity of the arguments presented in the previous chapter is demonstrated by the graphs shown in Fig. 5, where the relative signal intensity is plotted vs the relaxation time for a human patient head slice. Although an attempt to attribute the size of structures has not been made quantitatively, it is obvious, that the sharper structures of the skin are more attenuated than more extended structures inside the head for equal T_2. The images, from which the figures are taken, are shown in Figs. 6a–c. T_2 values were calculated from 12 echoes in a conventional multiecho 2D FT sequence.

A comparison of the single acquisition image (Fig. 5b) with a RARE image taken with 16 acquisitions (Fig. 5c) shows, that the T_2 contrast is much stronger in the single acquisition image. It is obvious as well, that the single acquisition image has sufficient resolution to be a valuable tool for patient positioning. More than that, due to its T_2 character it is especially suited to detect lesions with long T_2.

From a clinical point of view it is most important to note that the RARE sequence delivers images which are practically free from artifacts if an appropriate phase-encoding scheme is chosen. This is markedly different from the situation one encounters when echo imaging is applied to a back-projection imaging scheme (*16*).

DISCUSSION

Since its implementation in October 1984, we have examined about 1100 patients with RARE imaging in our department. We have found, that it is an indispensable tool for exact patient positioning. Above that, more than 90% of lesions in the head, which were lesions with long T_2, were clearly shown in the RARE imaging alone. Multiple sclerosis plaques are shown clearly in the RARE image. Combined with multislice techniques, a head scan with 8 slices can be performed in less than 2 min, leading to very short overall investigation times per patient. Due to the fact that the RARE sequence, which has proven to be most useful in head investigations and which is represented by Fig. 6c, gives only low T_2 contrast between medium T_2 values (200 ms and more), fat around the spinal chord is not always clearly distinguishable from tumors and therefore different sequences giving sharper contrast have to be tailored

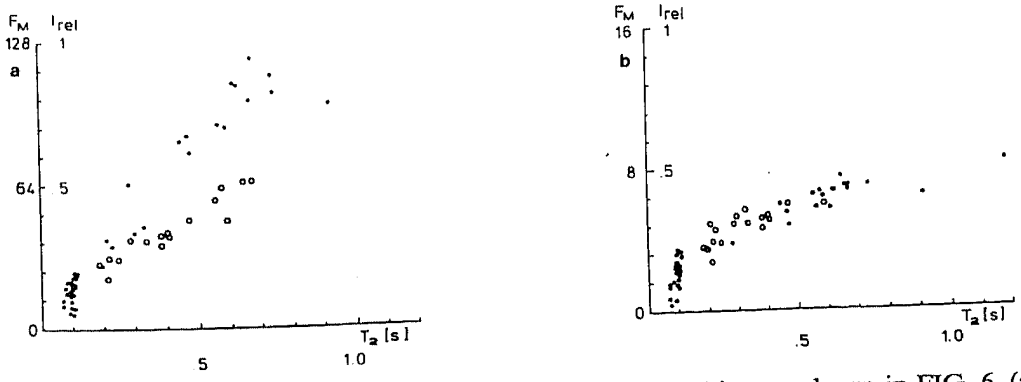

FIG. 5. Rel. intensities I_{rel} and figures of merit F_M vs T_2 for RARE images shown in FIG. 6. (a) Single-shot experiment; (b) 16-excitation experiment. Open circles correspond to sharp structures.

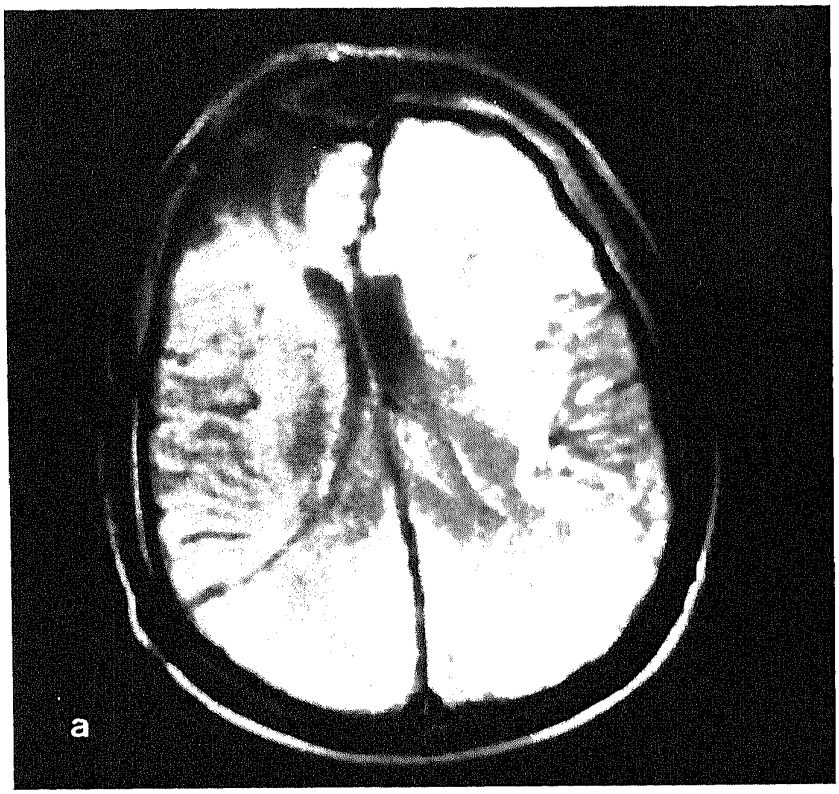

FIG. 6. Conventional 2D FT image (a) compared to a single-shot RARE image (b) and a 16-excitation RARE image (c) of a patient with recurrent pituitary adenoma with infiltration of the brain tissue. Imaging parameters for the conventional image were 1800 ms for the repetition time, echo readout time 33 ms.

for these applications. The single acquisition experiment (Fig. 6b) promises to be most useful in these cases (*18*).

In the abdomen, where the prediction of relaxation times is most difficult and short T_2 are not uncommon, the choice of the appropriate RARE sequence is often difficult—as is the choice of the appropriate conventional 2D FT experiment. RARE can be used here as a fast means to check for the T_2 sensitivity of a suspected lesion. According to the contrast of the RARE image one can choose the 2D FT sequence most likely to yield a good presentation of the lesion with more confidence, so that the overall efficiency and speed of an examination is increased even if the RARE image gives only poor lesion contrast.

The high signal sampling efficiency of RARE promises to make it a good method for 3D FT. Apart from that, it can be used to acquire images with very high S/N in reasonable time by averaging. Both possibilities are studied at the moment in our department.

EXPERIMENTAL

All our experiments were performed on a 0.23-T system Bruker BNT 1100. Patients were investigated using a 60-cm body coil, a 50-cm body coil, 28 and 22 cm head coils, and various surface coils for special cases. No special setup procedures were

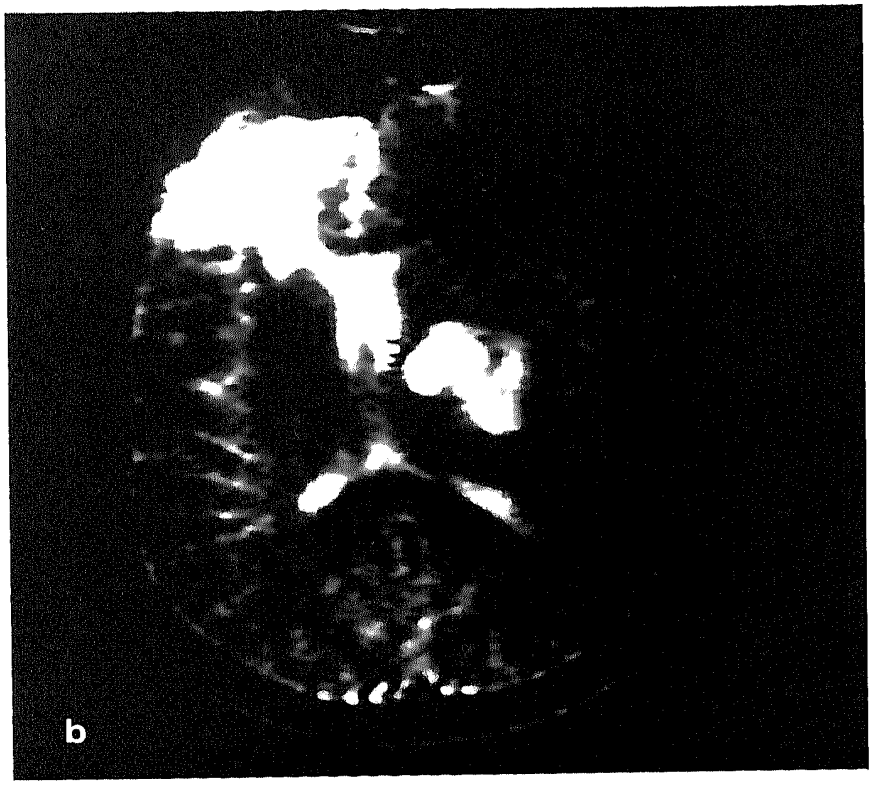

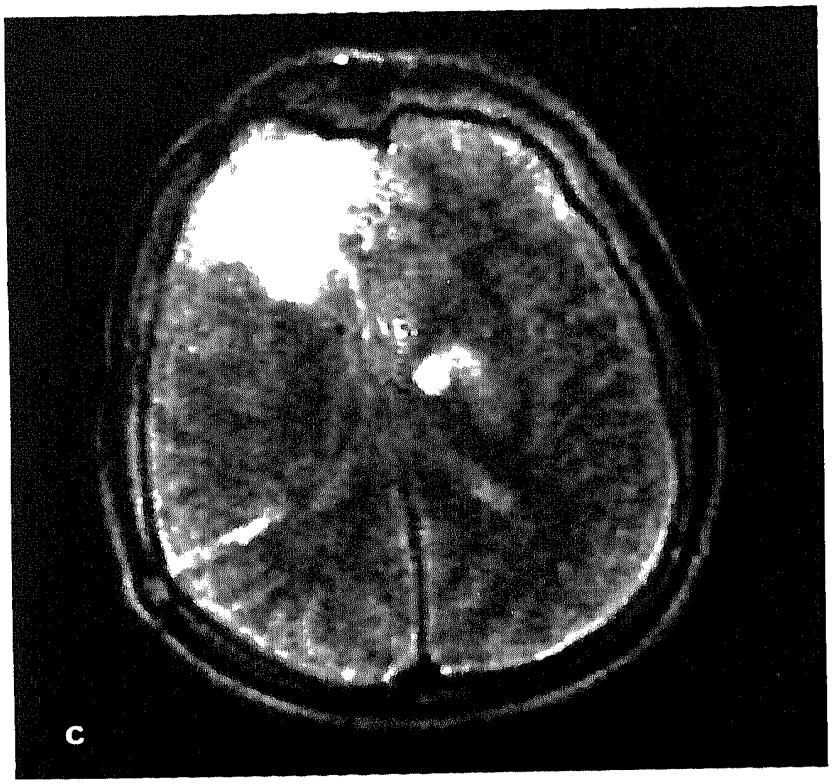

FIG. 6—*Continued.*

necessary for imaging with our method, allowing us to apply it as part of our routine measurement menu.

Slice width was 8 mm standard; some investigations were performed with down to 2 mm width. 2D FT and RARE imaging were taken without patient dislocation to allow the direct comparison of images.

APPENDIX

Explicit Evaluation of the Shape Function of a Lorentzian Image with RARE Imaging

A structure with Lorentzian spin-density distribution oriented along the phase-encoding gradient and symmetrical around the gradient field zero point yields in a 2D FT imaging sequence an echo for the second Fourier transformation which can be described as

$$E = M_0 \exp(a \cdot \varphi) \qquad \text{for} \qquad \varphi < 0$$

$$E = M_0 \exp(-a \cdot \varphi) \qquad \text{for} \qquad \varphi > 0$$

where φ, the time coordinate in a normal 1D FT experiment, is given by the dephasing gradient as described by Ernst (*17*). Fourier transformation yields the well-known function

$$G(\omega) = 2 \frac{aM_0}{a^2 - \omega^2} \qquad [1]$$

where ω is the spatial coordinate in frequency units. To calculate the lineshape according to a RARE imaging experiment, one has to multiply the echo function E with the relaxation function. The zero point of both functions needs not to be identical.

The time variable of the relaxation function has to be transformed into the time domain of the phase-encoding gradient. This can be done easily if one takes into account that the dwell time of the phase-encoding gradient steps has to be identified with the echo spacing $2\tau_e$. Due to the symmetry of the 2D FT algorithm, the dwell time of the phase encoding can be set equal to the dwell time dw of the data sampling for a geometrically square image. This leads to a compression of the timescale for the relaxation by a factor $2\tau_e/dw$ for a single shot experiment or $2\tau_e/(n \cdot dw)$ if one samples data in n acquisitions in the interleaving manner described above. This yields

$$E' = M_0 \exp\left(-\frac{2\tau_e}{n \cdot dw \cdot T_2}\right) \exp(a(\varphi - \varphi_0)) \qquad \text{for} \qquad \varphi < \varphi_0$$

$$E' = M_0 \exp\left(-\frac{2\tau_e}{n \cdot dw \cdot T_2}\right) \exp(-a(\varphi - \varphi_0)) \qquad \text{for} \qquad \varphi > \varphi_0.$$

Fourier transformation gives

$$G = \frac{M_0}{a - \frac{2\tau_e}{n \cdot dw \cdot T_2} - i\omega} \exp\left(\left(-\frac{2\tau_e}{n \cdot dw \cdot T_2} + i\omega\right)\varphi_0\right)$$

$$+ \frac{M_0}{a + \frac{2\tau_e}{n \cdot dw \cdot T_2} - i\omega} \exp\left(\left(-\frac{2\tau_e}{n \cdot dw \cdot T_2} + i\omega\right)\varphi_0\right)$$

$$- \frac{M_0}{a - \frac{2\tau_e}{n \cdot dw \cdot T_2} - i\omega} \exp(-a \cdot \varphi_0).$$

φ_0 represents the dephasing zero point, that is, the center of the "echo" E'.

Neglecting the first-order phase distortion factor $\exp(-i\omega\varphi_0)$ this can be described as the sum of three functions. The real part of the first term gives a Lorentzian line sharpened by $2\tau_e/(n \cdot dw \cdot T_2)$ compared to (1) and the real part of the second term gives a Lorentzian line broadened by the same term. The amplitude of both functions is attenuated by $\exp((-2\tau_e\varphi_0/(n \cdot dw \cdot T_2))$. The third term gives the loss of the signal due to the cutoff of the echo at $\varphi = 0$. If $\varphi_0 = 0$ the first and third terms cancel and one gets the familiar solution of the Fourier transform of an FID. For sharp structures, where $a \ll 2\tau_e/(n \cdot dw \cdot T_2)$ the amplitude of the signal is directly proportional to $M_0 \cdot T_2$, giving an image identical in appearance to the product of a spin-density image with a T_2 image as calculated from a multiecho sequence.

REFERENCES

1. T. F. BUDINGER, *IEEE Trans. Nucl. Sci.* **26,** 2812 (1979).
2. J. P. R. JENKINS, J. C. WATERTON, H. G. LOVE, X. P. ZHU, I. ISHERWOOD, AND D. ROWLANDS, *Br. Heart J.* **53,** 91 (1985).
3. P. VAN DIJK, Proceedings, Fourth Annual Meeting of the Society for Magnetic Resonance in Medicine, 1985, p. 572.
4. A. HAASE, J. FRAHM, D. MATTHAEI, W. HAENICKE, AND K. D. MERDOLDT, Proceedings, Fourth Annual Meeting of the Society for Magnetic Resonance in Medicine, 1985, p. 980.
5. P. MANSFIELD AND A. A. MAUDSLEY, *J. Magn. Reson.* **27,** 101 (1977).
6. R. J. ORDRIDGE, P. MANSFIELD, M. DOYLE, AND R. E. COPELAND, *Br. J. Radiol.* **55,** 729 (1982).
7. P. MANSFIELD, *Br. Med. Bull.* **40,** 187 (1984).
8. W. A. EDELSTEIN, U.S. Patents Nos. 4 451788, 4 431 968, 4 471 306.
9. Z. H. CHO, H. S. KIM, H. B. SONG, AND J. CUMMINGS, *Proc. IEEE* **70,** 1152 (1982).
10. E. M. HAACKE, F. H. BEARDEN, AND J. R. CLAYTON, Proceedings, Fourth Annual Meeting of the Society for Magnetic Resonance in Medicine, 1985, p. 978.
11. C. M. J. VAN UIJEN, *Magn. Reson. Med.* **18,** 268 (1984).
12. S. MEIBOOM AND D. GILL, *Rev. Sci. Instrum.* **29,** 688 (1958).
13. B. STROEBEL AND D. RATZEL, U.S. Patent pending.
14. A. MEHLKOPF, P. VAN DER MEULEN, AND J. SMIDT, *Magn. Reson. Med.* **1,** 295 (1984).
15. I. R. YOUNG AND M. BURL, UK Patent Appl. GB 2056078 A.
16. L. D. HALL AND S. SUKUMAR, *Magn. Reson. Med.* **18,** 179 (1984).
17. A. KUMAR, D. WELTI, AND R. ERNST, *J. Magn. Reson.* **18,** 69 (1975).
18. J. HENNIG, H. FRIEDBURG, AND B. STROEBEL, *J. Comput. Assist. Tomogr.* **10,** 375 (1986).